

Geological Society, London, Special Publications

## **3D discrete kinematic modelling applied to extensional and compressional tectonics**

T. Cornu, F. Schneider and J. -P. Gratier

*Geological Society, London, Special Publications* 2003; v. 212; p. 285-294  
doi:10.1144/GSL.SP.2003.212.01.19

---

**Email alerting service**      [click here](#) to receive free email alerts when new articles cite this article

**Permission request**      [click here](#) to seek permission to re-use all or part of this article

**Subscribe**      [click here](#) to subscribe to Geological Society, London, Special Publications or the Lyell Collection

---

### **Notes**

**Downloaded by**      on 11 June 2007

---

# 3D discrete kinematic modelling applied to extensional and compressional tectonics

T. CORNU<sup>1</sup>, F. SCHNEIDER<sup>1</sup> & J.-P. GRATIER<sup>2</sup>

<sup>1</sup>IFP, 1–4 avenue de Bois-Préau, 92500 Rueil-Malmaison, France (e-mail: tristan.cornu@ifp.fr; frederic.schneider@ifp.fr)

Present address: Faculty of Earth and Life Sciences, Tectonics, Vrije Universiteit, De Boelelaan 1085, 1081 HV Amsterdam, The Netherlands (e-mail: tristan.cornu@falw.vu.nl)  
<sup>2</sup>LGIT, Observatoire de l'Université de Grenoble, IRIGM, BP 53, 38041 Grenoble, France (e-mail: Jean-Pierre.Gratier@obs.ujf-grenoble.fr)

**Abstract:** The 3D simulation of coupled backward and forward deformation of geological layers is a new step in basin modelling. Although this problem could be addressed with either mechanical or kinematic approaches, the mechanical approach remains too complex to be addressed properly. The kinematic model described here allows a geologically valid path, which takes into account an incremental evolution in time. To obtain a better description of 3D geometries, the model uses a full hexaèdric discretization and the discrete neutral surface of each layer is used when performing the flexural slip deformation. An application to a synthetic geological case is then proposed, to study the behaviour of the structure in compressional and extensional contexts.

Modelling the evolution and petroleum potential of sedimentary basins is a complex problem, involving two distinct steps: (1) the simulation of the tectonic deformation, and (2) the computation of the hydrocarbon generation and migration. Until now, most basin modelling tools were constructed to address only one of these problems (Schneider & Wolf in press; Zoetmeyer 1992). A first attempt to couple deformation and fluid flow simulations was done recently (Schneider *et al.* 2000) but it is still limited to 2D cases with relatively simple kinematic patterns (vertical shear mechanism). The model we propose here is a discrete model for 3D flexural slip deformation (or mixed flexural slip and vertical shear), where further computations to solve fluid flow simulations might be done by using the mesh of the deformed elements.

Two distinct approaches can be chosen to model the tectonic deformations that occur in a sedimentary basin: (1) a mechanical approach, or (2) a kinematic approach. The mechanical approach has already been tested on analytical or geological cases (Barnichon 1998; Niño *et al.* 1998; Erickson and Jamison 1995; Bourgeois 1997; Coussy 1995). However, these studies were done on 2D cases with simplified assumptions on the mechanical behaviour of the rocks. 3D mechanical modelling that would include all the parameters relevant to natural deformation has never yet been proposed.

This may be explained by the extreme complexity of the mathematical formulation and computer limitations on one hand, and on the other hand, by the complexity of the phenomenon at geological time and space scales (Ramsay & Huber 1987), which makes it difficult to find the adapted rheological laws and boundary conditions. Even a model like 3DEC (Cundall 1988; Hart *et al.* 1988) is limited by its restrictive hypothesis of incremental deformation within deformed blocks, which is not realistic for natural deformation of sedimentary basins.

To overcome the difficulty of the mechanical approach, geologists have instead focused on the kinematic approach (Dahlstrom 1969), which is the geometrical translation of mechanical assumptions. Kinematic modelling is a good alternative, which can be sufficiently representative of the natural processes. A discrete approach (Waltham 1989, 1990; Diviès 1997) can also be used for further computation of thermal and fluid transfers, integration of rock attributes (i.e. porosity, permeability, thermal conductivity, etc.), and simulation of natural processes (i.e. sedimentation, erosion, and compaction). One limitation of the existing kinematic approaches is that the proposed models relate either to forward modelling (Suppe 1983; Gibbs 1983; De Paor 1988a, b; Contreras and Suter 1990) or to backward restoration (Moretti 1989; Gratier

*et al.* 1991; Gratier & Guillier 1993; Bennis *et al.* 1991). Therefore the modelling of tectonic deformation relies on two types of models to solve the problem of restoration and deformation (Egan *et al.* 1998). However, the main limitation is that most of the kinematic models are 2D, or 'pseudo-3D' at best (Wilkerson & Medwedeff 1991; Shaw *et al.* 1994). These pseudo-3D models extend the area conservation to volume conservation, but are limited to cylindrical cases, built with topologically equivalent 2D sections. The main restriction is that the associated finite displacement must be parallel in map view. To overcome these problems, we have developed and present here a discrete algorithm that can be used both for backward and forward modelling, and that can be applied to real 3D cases. The method is applied to an analytical sedimentary basin with a lateral termination, derived from real field structures.

### The model

The assumptions used to describe the 3D flexural slip mechanism are first briefly presented. The model is supported by three main assumptions.

- (1) Each layer of the basin is assumed to be independent, and the sliding between the layers is supposed to be perfect.
- (2) As a general simplification, we assume that the thickness of the layer is preserved through the whole progressive deformation. Alternatively, thickness changes could be integrated if required.
- (3) Because the flexural-slip mechanism would preserve the length of the neutral line of a layer, we assume that the area of the neutral surface is also kept constant in 3D.

Layer slip and preservation of the layer thickness are the most commonly used assumptions in literature (Suppe 1983; Waltham 1989, 1990), and they are consistent with the geological observations of the deformation of so-called competent layers (Ramsay & Huber 1987). The last assumption is a mechanical one, as it relies on the flexural-slip mechanism and deals with the neutral surface of a layer, which is supposed to conserve its area through deformation (Ramsay & Huber 1987). This is a powerful and useful assumption since further calculation of the progressive deformation will be greatly simplified by the use of a surface instead of a volume.

We take a discrete modelling approach here, and implementation of the algorithm is done in C++. The geological objects are defined as follows.

1. The basin defines the entire geological area. It contains all the tectonic portion of the studied domain within its geometric boundaries.

2. The faults are defined as the main zones of discontinuity within the domain. They allow the subdivision of the basin into a discrete number of subdomains, and they are defined as triangulated surfaces.
3. Each subdomain of the basin constitutes an independent block, which is bordered by the faults (footwall, hanging-wall). Their frontiers are defined either by a fault or by the boundary of the basin.
4. The layers are the simplified geometric representation of the lithologic beds. They are discretized with hexaedric elements with eight vertices, and they support the deformation algorithm.

### Mathematical description

The first step of the modelling is to build a mesh: all the layers of each block are discretized in elements. The elements are height vertices hexaedric element, with six faces that are not always coplanar. After the definition of the geological domains, the motion of the basin is modelled through the displacement of each node of the neutral surface of the layers. The neutral surface is defined here as the median surface of the layer. It passes through the middle point of the 'vertical' edges of each hexaedric element (Fig. 1a).

#### Sliding support

The support of sliding is defined with faces of the element in each layer. For the first layer of the block, we use the base faces of the element, for the upper layer we use the roof faces of the previous layer, and for the lateral surface of sliding, we use the faces that coincide with the lateral imposed border. Each face is defined by four vertices, and we cut them into two triangles of three vertices. This allows us to define the surface of sliding as a  $C^1$  piecewise surface, or plane:

$$(P): \alpha x + \beta y + \gamma z + h = 0$$

where  $\alpha$ ,  $\beta$ ,  $\gamma$ ,  $h$  are defined with the coordinates of the three vertices.

#### Bisector plane

The bisector planes define the intersection of two planes, and they will help us to preserve the distance through the displacement. They are defined with the help of the coordinates of the two planes they cut.

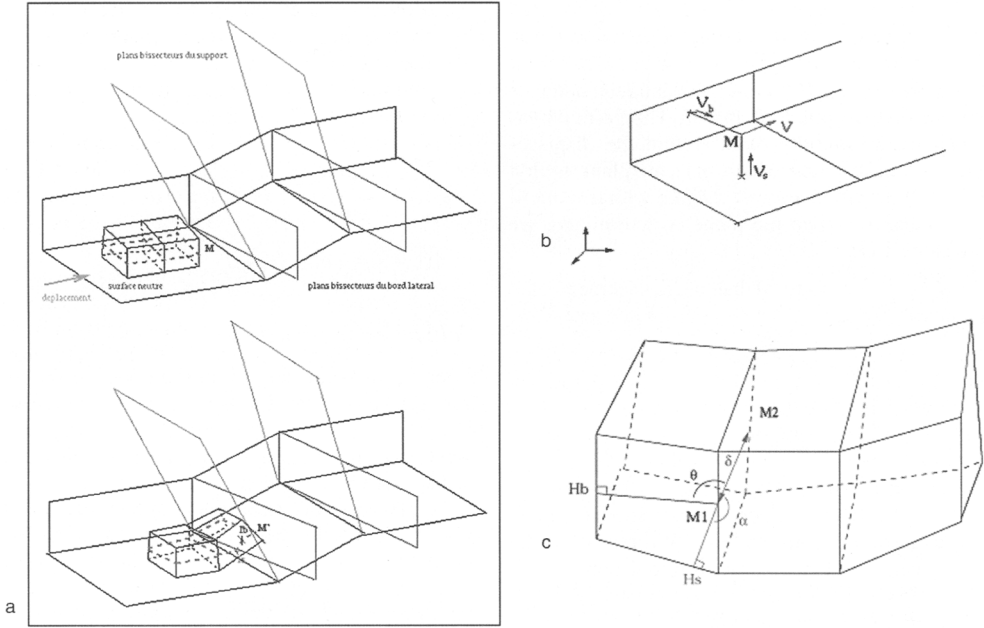


**Fig. 1.** (a) Diagram of the deformation of a layer with the algorithm based on neutral surface conservation; (b) diagram of the construction of the displacement direction for the bottom layer; (c) diagram of the construction of the displacement direction for the upper layers.

*Curvilinear displacement*

The movement of a neutral surface point is achieved with a curvilinear displacement  $\vec{I}_{\delta} \vec{v}$ , where  $\delta$  is the distance of displacement, and  $\vec{v}$  the direction of displacement. Due to the third space component, the direction of the displacement will depend not only on the basement, but also on the lateral border. We define  $\vec{v}$  as:

$$\vec{v} = \vec{n}_s \wedge \vec{n}_b$$

where  $\vec{n}_s$  is the normal vector of the support on which the layer slips, and  $\vec{n}_b$  the normal vector of an imposed lateral surface (Fig. 1b).

The definition of  $\vec{v}$  imposes to the displacement to be parallel both to the support and to the imposed lateral border. This first approximation provides a conservation of the width of the layer (the distance between each point of the neutral surfaces and the lateral boundary).

*Displacement step of a neutral surface node*

$M_0(x_0, y_0, z_0)$  is a node of the neutral surface. It is displaced following the draw  $D(M, \vec{v})$ :

$$D: \begin{cases} x_0 + v_x t \\ y_0 + v_y t \\ z_0 + v_z t \end{cases}$$

The point  $M_0$  follows (D) until it intersects one the bisector plane that split the domain. ( $P_{Bs}$ ) is a bisector plane of the basement, ( $P_{Bb}$ ) is a bisector plane of the lateral imposed border, defined by:

$$(P_{Bs}): \alpha_{bs} x + \beta_{bs} y + \gamma_{bs} z + h_{bs} = 0$$

$$(P_{Bb}): \alpha_{bb} x + \beta_{bb} y + \gamma_{bb} z + h_{bb} = 0$$

The coordinates of  $I_i = (D) \cap (P_{Bi}, i = b, s)$ , intersection point of (D) and the bisector plane ( $P_{Bi}$ ) are written:

$$I_i = \begin{cases} x_0 + v_x t_i \\ y_0 + v_y t_i \\ z_0 + v_z t_i \end{cases}$$

The position of  $M_0$  relative to the bisector planes is not known a priori, so we are obliged to calculate the two intersection points, with the following definition of  $t_i$ :

$$t_{ii} = \frac{-(\alpha_{bi}x_0 + \beta_{bi}y_0 + \gamma_{bi}z_0 + h_{bi})}{\alpha_{bi}v_x + \beta_{bi}v_y + \gamma_{bi}v_z}$$

We suppose  $d_i = \|MI_i\|$  to be the Euclidean distance between the two points  $I_i$  and  $M$ . The point  $M$  has to displace an amount of  $\delta$ . Before the displacement, we must define which bisector plane is first cut by ( $D$ ). It will be nearest the one with the smallest distance  $d_i$ . When the plane is determined, we have three cases:

- (1)  $d_i > \delta$ : the point  $M$  has a displacement of  $\delta$  along ( $D$ ), and its new coordinates are:

$$M = \begin{cases} x_0 + v_x \delta \\ y_0 + v_y \delta \\ z_0 + v_z \delta \end{cases}$$

- (2)  $d_i = \delta$ : the point  $M$  is the same than point  $I_i$ .  
 (3)  $d_i < \delta$ :  $M$  is displaced to  $I_i$ , but it still must displace a distance  $\delta - d_i$ . We repeat all the precedent operations, with initial point  $I_i$  and a new definition of  $\vec{v}$  according to the basement and the lateral border.

### Reconstruction of upper layers

The reconstruction of the upper layers tries to rebuild a geometry which conserves the angular and distance relationships of the previous step configuration. The complexity of the reconstruction comes from the parameters we have to define: the distance  $\delta$  between two nodes of the neutral surface, and two angles  $\alpha$  and  $\theta$  relative to the basement and to the lateral border (Fig. 1c).

$M_1$  and  $M_2$  are two successive points of the neutral surface:  $\delta = \|M_1M_2\|$ .  $H_s$  and  $H_b$  are the normal projection of  $M_1$  upon the basement and upon the lateral imposed border:

$$\cos \alpha = \frac{M_1\vec{M}_2 \cdot M_1\vec{H}_s}{\|M_1\vec{M}_2\| \|M_1\vec{H}_s\|}$$

$$\cos \theta = \frac{M_1\vec{M}_2 \cdot M_1\vec{H}_b}{\|M_1\vec{M}_2\| \|M_1\vec{H}_b\|}$$

The direction of displacement  $\vec{v}$  must now be defined according to  $\alpha$  and  $\theta$ . To do this, we place ourselves in a reference system  $\mathfrak{R}(M_1, e_1, e_2, e_3)$ , where:

$$\vec{e}_1 = \frac{M_1\vec{H}_s}{\|M_1\vec{H}_s\|}$$

$$\vec{e}_2 = \frac{M_1\vec{H}_b}{\|M_1\vec{H}_b\|}$$

$$\vec{e}_3 = \frac{M_1\vec{H}_s \wedge M_1\vec{H}_b}{\|M_1\vec{H}_s \wedge M_1\vec{H}_b\|}$$

We can define  $\vec{v}$  as:

$$\vec{v} = a\vec{e}_1 + b\vec{e}_2 + c\vec{e}_3$$

with:

$$\vec{v} \cdot \vec{e}_1 = \cos \alpha$$

$$\vec{v} \cdot \vec{e}_2 = \cos \theta$$

$$\|\vec{v}\| = 1 = \sqrt{a^2 + b^2 + c^2}$$

### Volume reconstruction

After the displacement of all the nodes of the neutral surface of a layer, we have to restore the volume of the layer. To perform this restoration, we use the vertical edges. Each node of the neutral surface belongs by definition to a vertical edge. Thus, after displacement, we rebuilt the volume by a rigid rotation of the vertical edge.

### Geological application

The test was done on a synthetic case. We constructed a geometric model (Fig. 2), which is similar to a field area in the Gulf of Mexico (Trudgill *et al.* 1999, fig. 2c; Rowan *et al.* 1999, fig. 31), or to Niger Delta structures (Crans *et al.* 1980). However, we are not trying to make any study of these areas, which are only named to help to figure what kind of application could be expected from the model. Such a structure contains both extensional and compressional structures, which result from gravity sliding processes. We assume the conservation of the global volume of the sediment (contained between the two main faults) during such a deformation. We also impose a lateral termination of the structure in order to model its lateral 3D evolution both in space and time. In this way, we can study the evolution of a part of a sedimentary basin ending along a non-vertical lateral ramp. With this experiment, we hope to get information on the 3D behaviour of the structure when it is subjected to gravity sliding. We will also study the local volume variations and the effect of the lateral ramp on the displacement field.

The limits (Fig. 2c) of the footwall are defined by a normal fault with a 20° dip at the rear, a reverse fault with a 20° dip at the front, and a lateral ramp with a 70° dip along one lateral boundary. The other lateral boundary is free. The hanging wall is a block of 11286 elements. The lithologic sequence is made up of a composite sequence of eleven layers of various thicknesses, to see the behaviour of the algorithm with different thicknesses. The length of the model is 35000 m, its width is 10000 m, and its thickness is 4450 m (Fig.

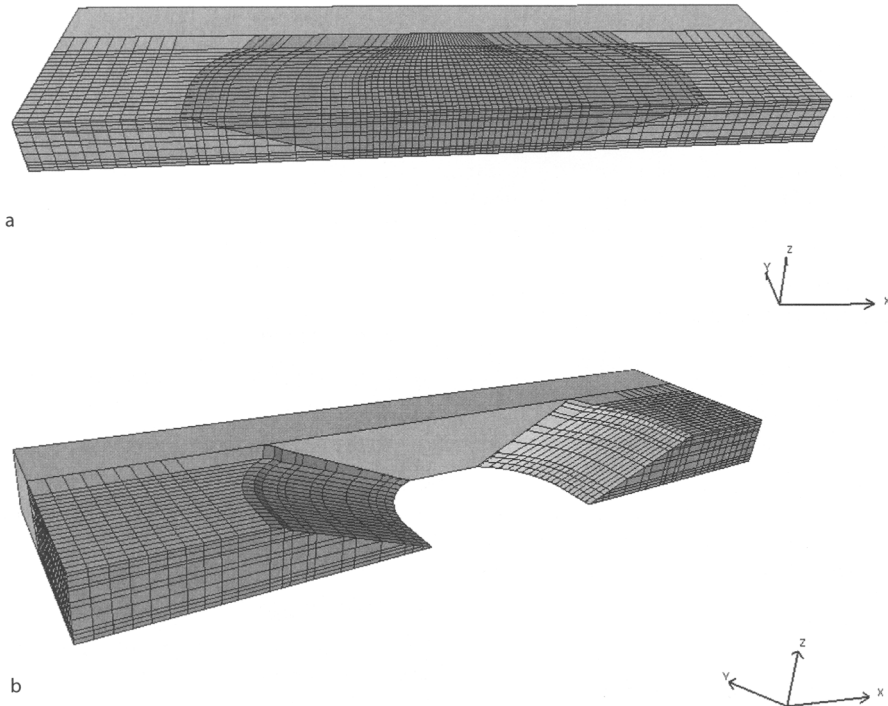


**Fig. 2.** (a) basin at the initial state; (b) description of the domain boundaries.

2b). The kinematic boundary condition is applied at the back of the hanging wall and imposes a displacement of 1000 m in the  $x$  direction at each time step. This means that all the elements of the first layer will move of 1000 m, and that those of the upper layers will be reconstructed according to the first layer deformation. All layers are supposed to deform by flexural slip, although it could also be possible to integrate other deformation mechanisms such as vertical shear for some layers. The footwall is supposed to be rigid, and is also discretized because its top helps to define the sliding support.

In Figure 3a–e we illustrate the evolution of the basin after four time steps and thus 4000 m of displacement. Below, we will outline our major observations.

### *Basin geometry*

The resulting geometry remains consistent with the initial shape, and displays no anomalous or unexpected deformations like crossing edges. The global volume variation of the hanging wall after deformation is lower than 1% or 2%. This is an acceptable and realistic result. It implies that even if the volume conservation was not an independent constraint, the coupled assumptions made on the

neutral surface and on the edge rebuilding were relevant.

### *Transport direction*

In Figure 4a, the components of displacement for each node of the neutral surface are projected onto a horizontal plane. In that their direction varies widely in map view, we can conclude that our modelled deformation is fully 3D.

### *Boundary effects*

The lateral displacements observed on the free vertical boundary (Fig. 4b, c) show the effect of a lateral ramp as a geometrical boundary condition. The displacement values are dependent on the direction and dip of the imposed lateral boundary as shown on Figure 4, and also on the thickness of the layers. They document the incidence of the geometry of a lateral termination on the kinematic evolution of the basin. Moreover, we suggest that lateral bedding slip or lateral flexural-slip deformation might act as evidence for a lateral termination, provided we could observe these features directly in the field.

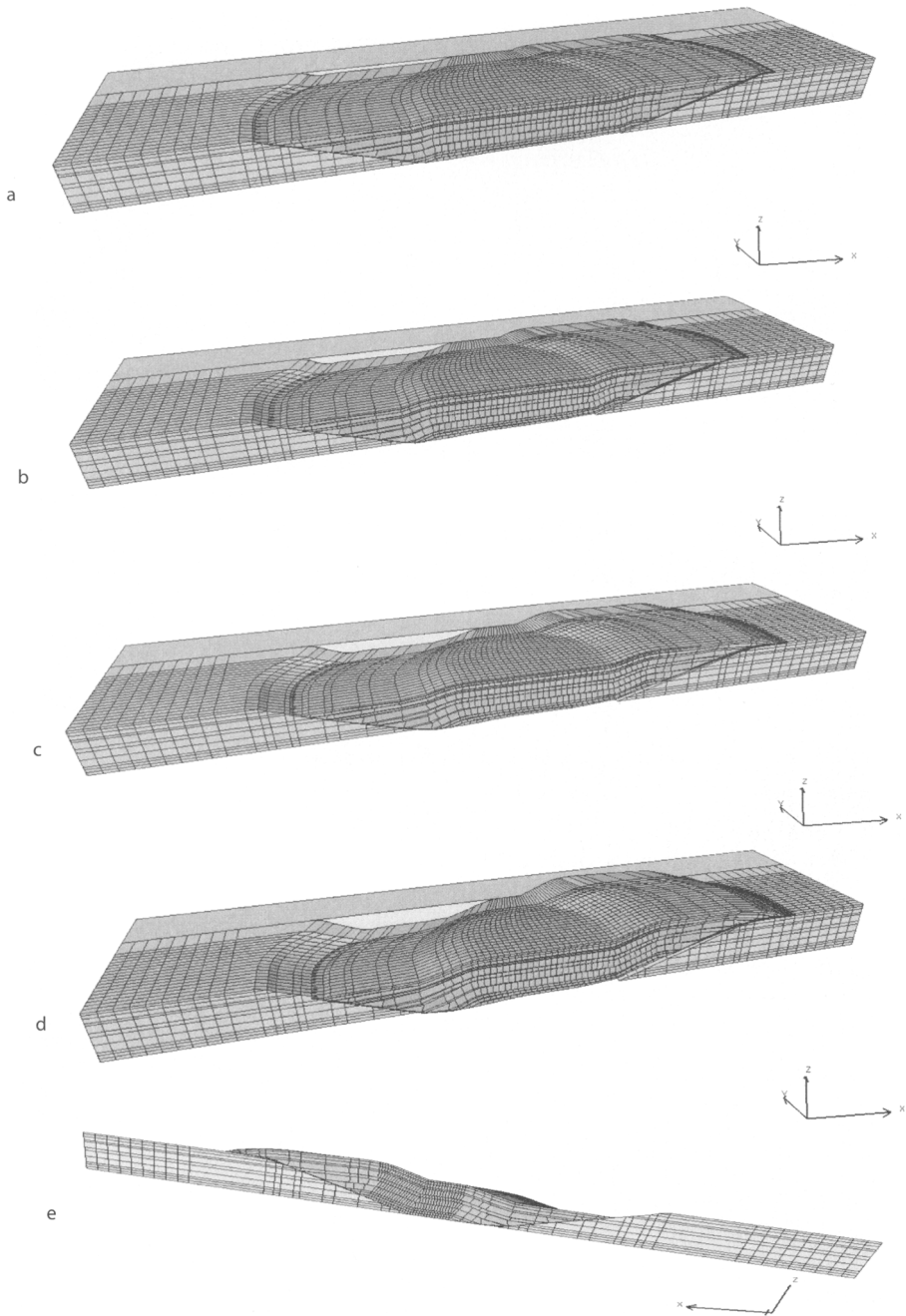


**Fig. 3.** (a) View of the deformed basin after 1000 m of displacement; (b) view of the deformed basin after 2000 m of displacement; (c) view of the deformed basin after 3000 m of displacement; (d) view of the deformed basin after 4000 m of displacement; (e) inverted view from the lateral imposed boundary of the deformed basin after 4000 m of displacement.

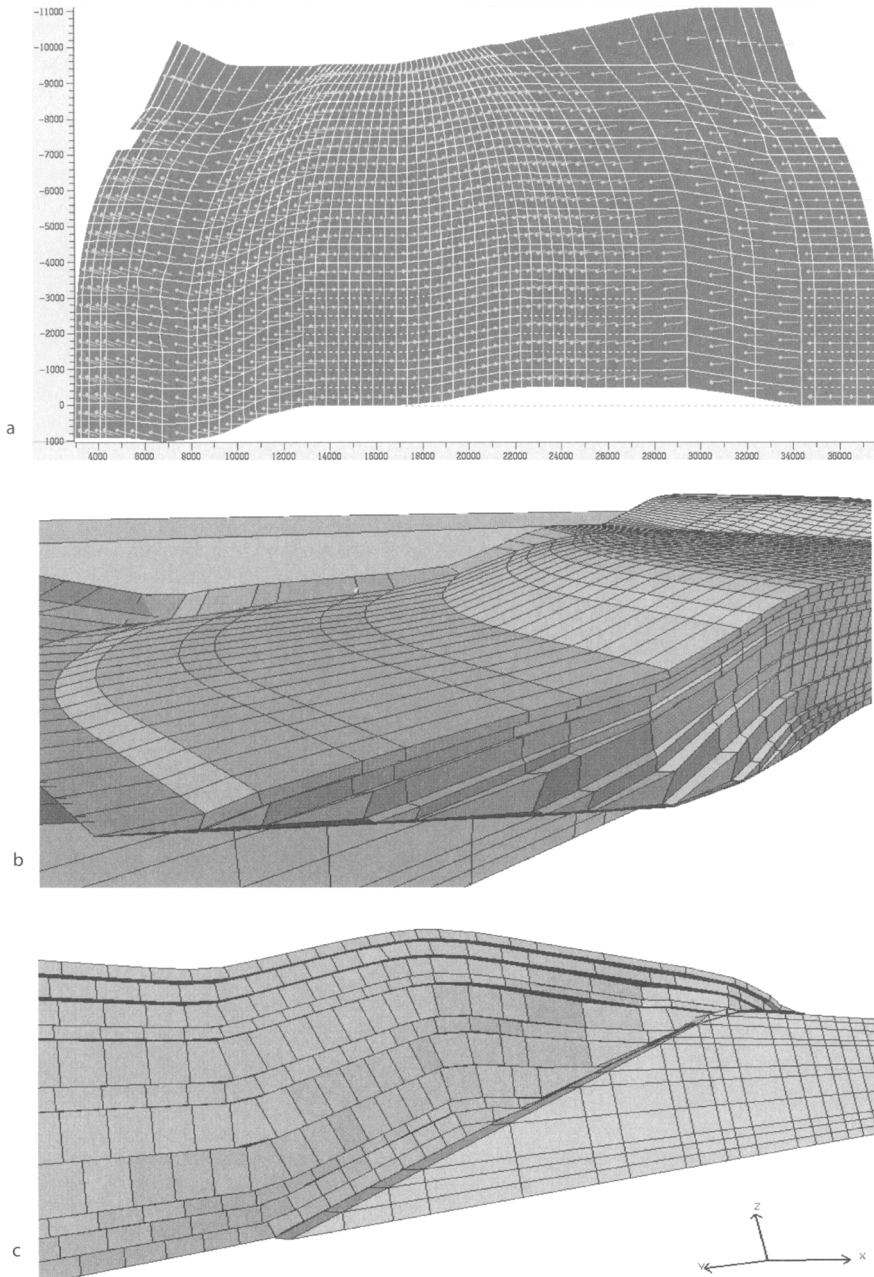


**Fig. 4.** (a) Map of the vertical projection on an horizontal plane of the neutral surface node displacement components, after 4000 m of displacement; (b) zoom of the lateral displacements observed on the normal fault after 4000 m of displacement; (c) zoom of the lateral displacements observed on the reverse fault after 4000 m of displacement.

#### *Local volume variation*

Here, the local volume variation will be designed by  $\Delta V_i/V_i$ , with  $\Delta V_i = V_{initial} - V_{final}$ . According to literature, internal strain data must usually be taken

into account in 2D during balancing (Woodward *et al.* 1986; Mitra 1994; Mac Naught & Mitra 1996), but also in 3D when deformation is no longer planar (Von Winterfeld & Oncken 1995). In our results, the local volume variations are clearly

located in particular areas (Fig. 5a–d). Volume gain is observed for elements that cross the normal fault, whereas volume loss is observed for elements that cross the reverse fault. The geometric evolution of the elements can be tied to natural processes. If  $\Delta V_i/V_i$  is positive, the internal processes are responsible for a decrease of the element overlaps, with a mechanism that could relate to compaction (for example by pressure-solution (Gratier 1993), with the occurrence of stylolites in field samples). On the other hand, if  $\Delta V_i/V_i$  is negative, the internal deformation increases the amount of void space between the elements, and may be matched with micro-fracturing mechanisms such as open or sealed cracks in the field. These local variations are mainly caused by the geometric properties of the geological domain: basin morphology, fault architecture, blocks or layers. For example, volume variations are broadly correlated with the thickness of the layers. However, they still remain good indicators for the localization of highly strained zones. If we look at the evolution of  $\Delta V_i/V_i$  within the basin, we see that the maximal negative values are located near the hinge zone of the fault-bend folds, where the curvature of the ramp is maximum. We also see a relative attenuation of the  $\Delta V_i/V_i$  when getting farther from the curvature.

### Normal fault geometry

The dip of the normal fault is clearly too low when compared with natural faults. We could have increased the dip of the faults; however, due to the discrete procedure, this dip must evolve progressively along the entire fault in the same way as for listric faults. Such a complex geometry was not tested here for simplicity.

### Conclusion

The model presented here is a discrete kinematic model, which offers the opportunity to work both in extensional and compressional domains or coupled ones. This type of modelling is a first step in order to couple tectonic deformation modelling with the computation of fluid flow or hydrocarbon migration during progressive deformation. It is also a strong tool to study complex geological problems, even given that simplifications of the geometries may be required. It will ideally lead to a better understanding of the mechanism of internal strain, and to a better representation of localization of strain in three dimensions.

The quantitative values of the computed parameters, such as the local volume variation or the

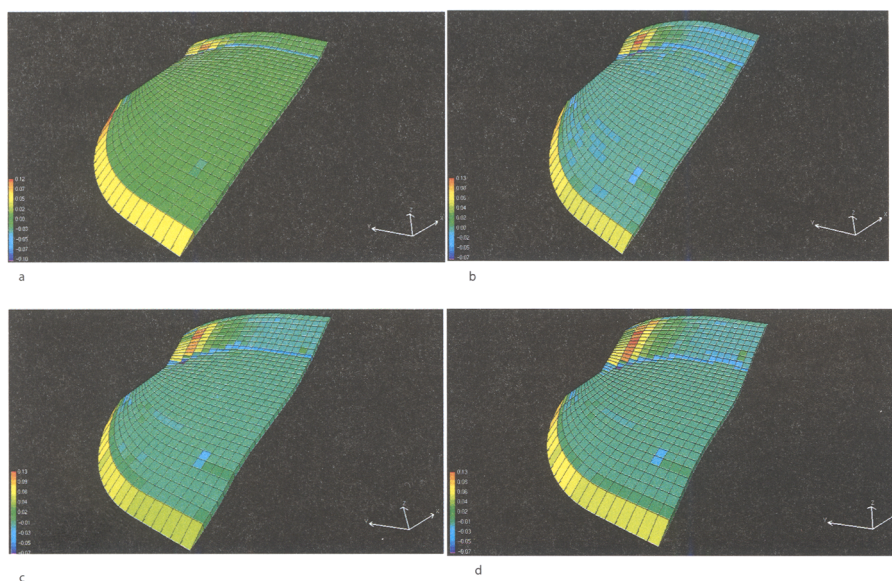


**Fig. 5.** The legend on the left of each picture corresponds to the  $\Delta V_i/V_i$ . (a) View of the local variation of volume on the first layer after 1000 m of displacement; (b) view of the local variation of volume on the first layer after 2000 m of displacement; (c) view of the local variation of volume on the first layer after 3000 m of displacement; (d) view of the local variation of volume on the first layer after 4000 m of displacement.

displacement directions, are strongly dependent on the geometry of the heterogeneous domains (faults, blocks and layers). Although the limitation of the computational scheme may restrict the numbers of layers, this is a feature common to all numerical models. Nevertheless, we believe that computed geometric and kinematic parameters should be used as semi-quantitative indicators of strain, thus allowing for comparison between 3D numerical modelling and field structures. In addition, systematic testing of the effect of the various parameters should provide general kinematic laws on the links between all these parameters, and guide further field study towards the most significant markers of the deformation (i.e. pressure-solution or fractures), both in the reservoir rock potential and seals.

## References

- BARNICHON, J. D. 1998. *Finite element modelling in structural and petroleum geology*. PhD thesis, Université de Liège.
- BENNIS, C., VEZIEN, J. G. & IGLESIAS, G. 1991. Piecewise surface flattening for non-distorted texture mapping. *Computer Graphics*, **25**(4), 237–246.
- BOURGEOIS, E. 1997. *Mécanique des milieux poreux en transformation finie: formulation des problèmes et méthodes de résolution*. PhD thesis, Ecole Nationale des Ponts et Chaussées.
- CONTRERAS, J. & SUTER, M. 1990. Kinematic modelling of cross-sectional deformation sequences by computer simulation. *Journal of Geophysical Research*, **95**, 21913–21929.
- CRANS, W., MANDL, G. & HAREMBOURE, J. 1980. On the theory of growth faulting: a geometrical delta model based on gravity sliding. *Journal of Petroleum Geology*, **2**, 265–307.
- COUSSY, O. 1995. *Mechanics of Porous Continua*. Wiley, London.
- CUNDALL, P. A. 1988. Formulation of a three-dimensional distinct element model-part I. A scheme to detect and represent contacts in a system composed of many polyhedral blocks. *International Journal of Rock Mechanics, Mineral Science & Geomechanical Abstracts*, **25**(3), 107–116.
- DAHLSTROM, C. D. A. 1969. Balanced cross sections. *Canadian Journal of Earth Sciences*, **6**, 743–757.
- DE PAOR, D. G. 1988a. Balanced section in thrust belts, Part 1: construction. *AAPG Bulletin*, **72**(1), 73–90.
- DE PAOR, D. G. 1988b. Balanced section in thrust belts, Part 2: computerised line and area balancing. *Geobyte*, May, 33–37.
- DIVIÈS, R. 1997. *FOLDIS: un modèle cinématique de bassins sédimentaires par éléments discrets associant plis, failles, érosion/sédimentation et compaction*. PhD thesis, Université Joseph Fourier de Grenoble.
- EGAN, S. S. *et al.* 1998. Computer modelling and visualisation of the structural deformation caused by movement along geological faults. *Computers and Geosciences*, **25**, 283–297.
- ERICKSON, S. G. & JAMISON, W. R. 1995. Viscous-plastic finite-element models of fault-bend folds. *Journal of Structural Geology*, **17**, 561–573.
- GIBBS, A. D. 1983. Balanced cross-section construction from seismic sections in areas of extensional tectonics. *Journal of Structural Geology*, **5**, 153–160.
- GRATIER, J. P. 1993. Le fluage des roches par dissolution-cristallisation sous contrainte, dans la croûte supérieure. *Bulletin de la société géologique de France*, T. **164**(2), 267–287.
- GRATIER, J. P. & GUILLIER, B. 1993. Compatibility constraints on folded and faulted strata and calculation of total displacement using computational restoration (UNFOLD program). *Journal of Structural Geology*, **15**(3–5), 391–402.
- GRATIER, J. P., GUILLIER, B., DELORME, A. & ODONNE, F. 1991. Restoration and balance of a folded and faulted surface by best-fitting of finite elements: principles and applications. *Journal of Structural Geology*, **13**(1), 111–115.
- HART, R., CUNDALL, P. A. & LEMOS, J. 1988. Formulation of a three dimensional distinct element model-part II. Mechanical calculations for motion and interaction of a system composed of many polyhedral blocks. *International Journal of Rock Mechanics, Mineral Science & Geomechanical Abstracts*, **25**(3), 117–125.
- MAC NAUGHT, M. A. & MITRA, G. 1996. The use of finite strain data in constructing a retrodeformable cross-section of the Meade thrust sheet, southeastern Idaho, U.S.A. *Journal of Structural Geology*, **18**(5), 573–583.
- MITRA, G. 1994. Strain variation in thrust sheets across the Sevier fold-and-thrust-belt (Idaho-Utah-Wyoming): implications for sections restoration and wedge taper evolution. *Journal of Structural Geology*, **16**(4), 585–602.
- MORRETTI, I., WU, S. & BALLY, A. W. 1990. Computerized balanced cross-section LOCACE to reconstruct an allochthonous salt sheet, offshore Louisiana. *Marine and Petroleum Geology*, **7**, 371–377.
- NIÑO, F., CHÉRY, J. & GRATIER, J. P. 1998. Mechanical modelling of the Ventura basin: origin of the San Cayetano thrust fault and interaction with the Oak Ridge fault. *Tectonics*, **17**, 955–972.
- RAMSAY, J. G. & HUBER, M. I. 1987. *The Techniques of Modern Structural Geology - Volume 2: Folds and Fractures*. Academic Press, New York.
- ROWAN, M. G., JACKSON, M. P. A. & TRUDGILL, B. D. 1999. Salt-related fault families and fault welds in the northern Gulf of Mexico. *AAPG Bulletin*, **83**, 1454–1484.
- SCHNEIDER, F. & WOLF, S. 2000. Quantitative HC potentiel evaluation using 3D basin modelling: application to Franklin structure, central graben, North sea, U.K. *Marine and Petroleum Geology*.
- SCHNEIDER, F., WOLF, S., FAILLE, I. & POT, D. 2000. Un modèle de bassin 3D pour l'évaluation du potentiel pétrolier: application à l'offshore congolais. *Oil and Gas Science and Technology*.
- SHAW, J. H., HOOK, S. C. & SUPPE, J. 1994. Structural trend analysis by axial surface mapping. *AAPG Bulletin*, **78**, 700–721.
- SUPPE, J. 1983. Geometry and kinematic of fault-bend folding. *American Journal of Science*, **283**, 684–721.

- TRUDGILL, B. D., ROWAN, M. G., FIDUK, J. C. *et al.* 1999. The perdido fold belt, Northwestern Deep Gulf of Mexico, part 1: structural geometry, evolution and regional implications. *AAPG Bulletin*, **83**, 88–113.
- VON WINTERFELD, C. & ONCKEN, O. 1995. Non-plane strain in section balancing: calculation of restoration parameters. *Journal of Structural Geology*, **17**(3), 457–450.
- WALTHAM, D. 1989. Finite difference modelling of hanging wall deformation. *Journal of Structural Geology*, **11**, 433–437.
- WALTHAM, D. 1990. Finite difference modelling of sand-box analogues, compaction and detachment free deformation. *Journal of Structural Geology*, **12**, 375–381.
- WILKERSON, M. S. & MEDWEDEFF, D. A. 1991. Geometrical modelling of fault-related folds: a pseudo-three-dimensional approach. *Journal of Structural Geology*, **13**, 801–812.
- WOODWARD, N. B., GRAY, D. R. & SPEAR, D. B. 1986. Including strain data in balanced cross section. *Journal of Structural Geology*, **8**(3–4), 313–324.
- ZOETEMEIJER, R. 1992. *Tectonic modelling of forelands basins, thin skinned thrusting, syntectonic sedimentation and lithospheric flexure*. PhD thesis, Vrije Universiteit Amsterdam.